

## 4-nitrophenol Detection in Water Sample Using Linear Sweep Voltammetry with *f*-Multi Walled Carbon Nanotubes modified electrode

Raja Nehru<sup>1</sup>, Tse-Wei Chen<sup>1,2</sup>, Shen-Ming Chen<sup>1,\*</sup>, Tien-Wen Tseng<sup>2</sup>, Xiaoheng Liu<sup>3,\*</sup>

<sup>1</sup> Electroanalysis and Bioelectrochemistry Lab, Department of Chemical Engineering and Biotechnology, National Taipei University of Technology, No.1, Section 3, Chung-Hsiao East Road, Taipei 106, Taiwan, ROC.

<sup>2</sup> Departments of Chemical Engineering and Biotechnology, National Taipei University of Technology, Taipei 106, Taiwan (ROC)

<sup>3</sup> Key Laboratory of Education Ministry for Soft Chemistry and Functional Materials, Nanjing University of Science and Technology, Nanjing 210094, China.

\*E-mail: [smchen78@ms15.hinet.net](mailto:smchen78@ms15.hinet.net) (S.M.Chen); [xhliu@mail.njust.edu.cn](mailto:xhliu@mail.njust.edu.cn) (X.H. Liu)

Received: 22 March 2018 / Accepted: 12 May 2018 / Published: 5 July 2018

---

In this era, we report active carbon source (*f*-MWCNTs) with more electrode active surface area (EASA). The EASA is a significant role in batteries, supercapacitors and sensor application. Herein, we proposed modified electrode (GCE/*f*-MWCNTs) in the application of a sensor for the detection of 4-NP. The structural defects and morphological analysis were characterized by Raman spectroscopy and transmission electron microscopy (TEM), respectively. Moreover, the electron transfer properties of the modified electrode (GCE/*f*-MWCNTs) were analyzed by using Electrochemical Impedance Spectroscopy (EIS). The electrochemical sensor was developed based on prepared *f*-MWCNTs on a glassy carbon electrode (GCE). The electrocatalytic activity of (GCE/*f*-MWCNTs) modified electrode evaluated by the determination of 4-NP on cyclic voltammetry (CV) and linear sweep voltammetry (LSV). The proposed sensor exhibited good electrocatalytic activity towards the determination 4-NP in a water sample. In addition, the real sample analysis was carried out in laboratory tap water and obtained an acceptable recovery rate (97%), respectively.

---

**Keywords:** 4-nitrophenol, *f*-MWCNT, electrochemical determination, water sample

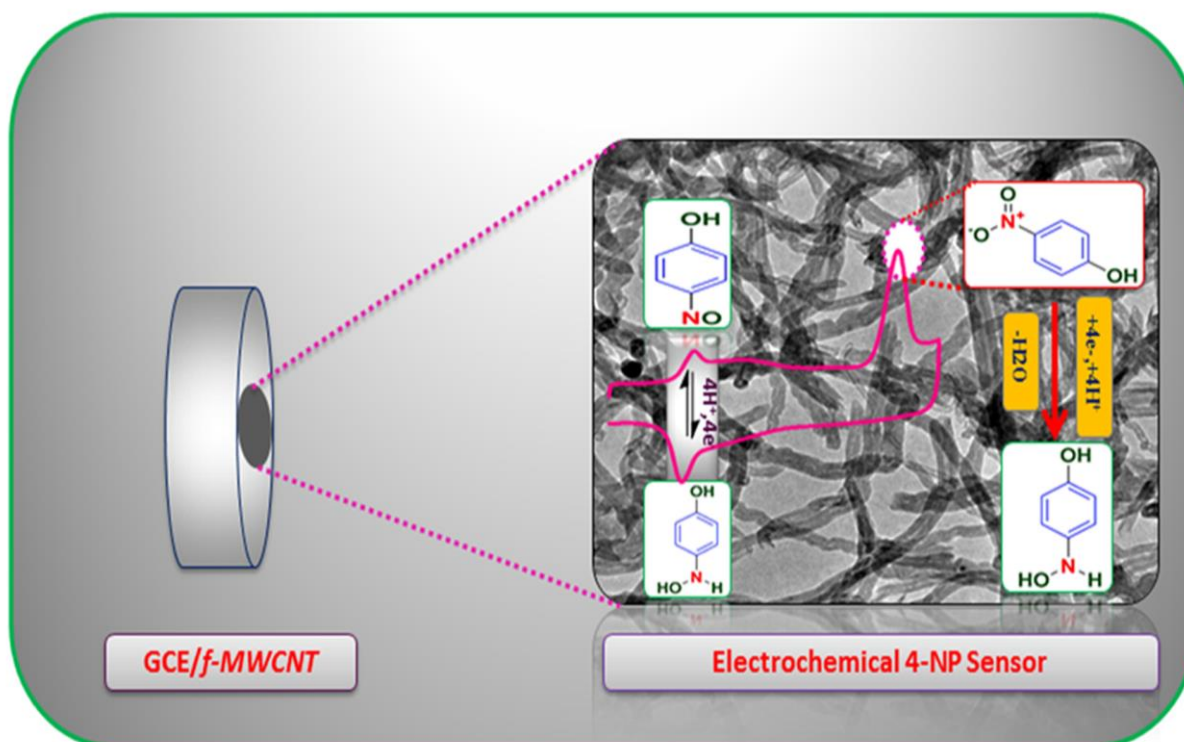
### 1. INTRODUCTION

Nitrophenols isomers are used in many industrial sectors such as pharmaceutical, agrochemical, petrochemical, textile, plastics, rubber, pesticides, and dyes production.[1-3] 4-NP has been found not only in industrial wastewater but also in a lake and seawater. In particular, the 4-nitrophenol has an

intensive toxic effect on methemoglobin formation, causing liver and kidney damage, anemia, skin and eye irritation, and systemic poisoning.[4-5] 4-nitrophenol is identified to be a priority pollutant by the US Environmental Protection Agency with an allowed limit of 60 ppb (0.43  $\mu\text{M}$ ) in drinking water.[6]

To date, numerous analytical methods such as mass spectrometry,[7] high-performance liquid chromatography(HPLC),[8-9] spectrophotometry,[10-12] fluorescence,[13-14] flow injection analysis,[15] and electrochemical methods.[16-21] The chemically modified electrodes offer special benefits such as a low detection limit with good sensitivity and stability besides minimized electrode fouling.[22] Carbon-based materials have been employed for various application such as batteries, and supercapacitors.[23-24] carbon nanotubes (CNTs) has its unique properties such as high electrical conductivity and high surface area. Moreover, it provides high sensitivity in electroanalysis and sensor developments.[25-26]

Herein, the carbon materials are the key factor in developing sensor. However, it has high conductivity and more surface area. We are moving forward to developing the electrode (GCE) active surface area (A). The proposed GCE/*f*-MWCNTs modified electrode offers good EASA (0.2756  $\text{cm}^2$ ). However, EASA of modified electrode calculated by Randles-Sevcik equation. In addition, we developed the modified (GCE/*f*-MWCNTs) electrode to detect 4-NP from a water sample. The developed modified electrode gives good electrocatalytic activity with good detection limit. Moreover, the developed sensor was analyzed by using laboratory tap water (LTW) and it gives an acceptable percentage (97%), respectively.



**Scheme 1.** schematic illustration of 4-nitrophenol detection on active surface species of modified electrode (GCE/*f*-MWCNTs)

## 2. EXPERIMENTAL

### 2.1 Materials and methods

Pure-MWCNTs, 4-Nitrophenol, Nitric acid ( $\text{HNO}_3$ ), Sulfuric acid ( $\text{H}_2\text{SO}_4$ ) disodium hydrogen phosphate ( $\text{Na}_2\text{HPO}_4$ ) and sodium dihydrogen phosphate ( $\text{NaH}_2\text{PO}_4$ ) were bought from Sigma Aldrich. The supporting electrolyte 0.05 M phosphate buffer solution (PBS) was prepared by using 0.05 M disodium hydrogen phosphate ( $\text{Na}_2\text{HPO}_4$ ) and sodium dihydrogen phosphate ( $\text{NaH}_2\text{PO}_4$ ), and pH of PBS was varied by adding  $\text{NaOH}/\text{H}_2\text{SO}_4$ . The pH measurements were carried out using pH meter (pH500). Double distilled (DD) water was used throughout the experimental work. All chemicals and reagents used in this study of analytical grade without additional purification.

The Carbon nanomaterials (MWCNTs) are a group of conducting materials. Here we present the function of hydrophilic behavior nature such as  $-\text{COOH}$  and  $-\text{OH}$  groups. Pure-MWCNTs were oxidized according to previously reported procedures.[27] The Pure-MWCNTs (0.5g) was dispersed into 50 ml (1:1 v/v) ratio of  $\text{HNO}_3$  (67%) and  $\text{H}_2\text{SO}_4$  (97%) and kept at 60 °C under magnetic stirring for 30 min. The obtained solution was subjected to ultrasonicated for 6 hrs and after completion of sonication process, the black solution kept at room temperature. Moreover, the black solution is washing and centrifuged (6000 rpm) several times using DD water up to pH-7. Finally, complete removal of acids from residual of the black solution and dried at room temperature. The obtained *f*-MWCNTs are further used for the preparation of modified electrode.

### 2.2 characterizations

The structural behavior of *f*-MWCNTs was evaluated by using Raman spectrum and TEM analysis. The electrochemical studies were carried out two different voltammetry techniques, cyclic voltammetry (CV) and linear sweep voltammetry which was performed CHI1205C workstation. The conventional three electrode systems are a GCE-working electrode, saturated  $\text{Ag}/\text{AgCl}$  (saturated  $\text{NaCl}$ )-reference electrode and platinum wire-counter electrode. All electrochemical measurements were fulfilled by room temperature.

### 2.3 Fabrication of modified electrode

The fabrication of modified electrode (GCE/*f*-MWCNTs) was prepared by 5 mg *f*-MWCNTs with the dispersion of 1 mL of DI water and then the homogeneous solution obtained from ultrasonication at 15 min. The 6  $\mu\text{L}$  well dispersed homogeneous solution of *f*-MWCNTs was drop cast on GCE electrode and dried at room temperature. This modified electrode (GCE/*f*-MWCNTs) was used for further electrochemical studies. The schematic representation of 4-NP detection shown in scheme 1.

### 3. RESULTS AND DISCUSSION

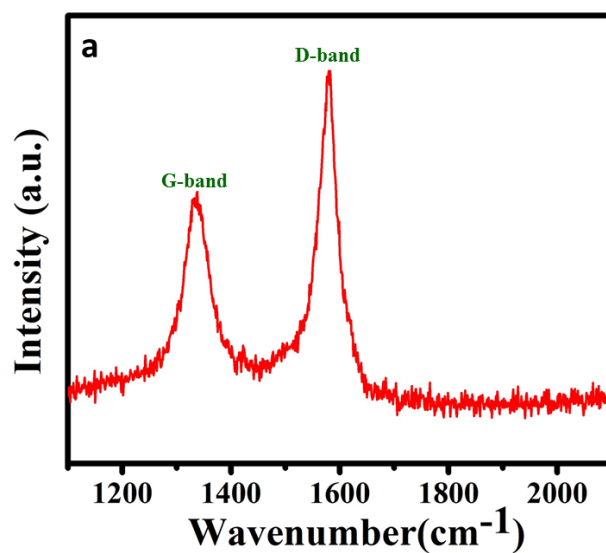


**Figure 1.** Raman spectrum of *f*-MWCNTs

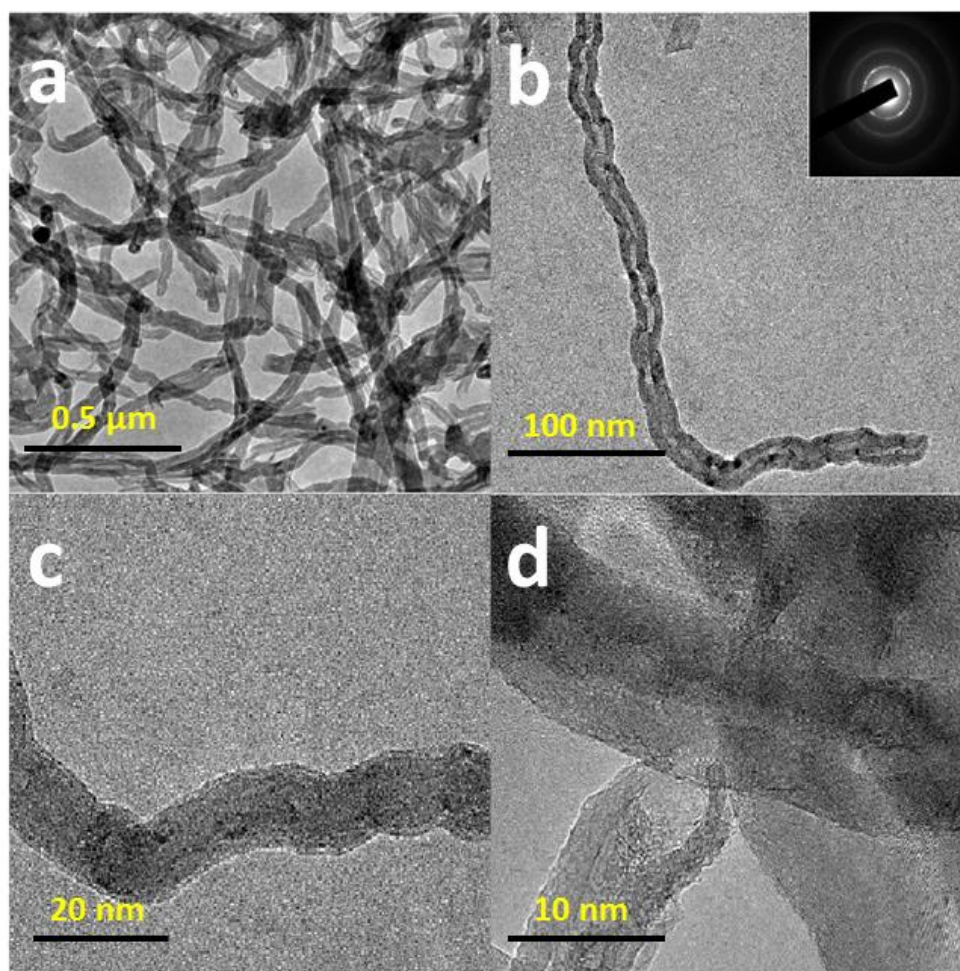


**Figure 2.** Different magnification TEM images of *f*-MWCNTs (a=0.5 μm, b=100 nm c=20 nm and d=10 nm).

The Raman spectroscopy is suitable tool to study the disorders nature of carbon materials, *f*-MWCNT, hence the *f*-MWCNT was identified by using Raman spectra. Figure. 1 shows Raman spectra of carbon materials (*f*-MWCNTs) which is displaying prominent two broad bands at 1344 and 1580  $\text{cm}^{-1}$ , such as D band (disordered) and G band (graphitic) respectively.[28] The relative intensities ratio ( $I_D/I_G$ ) of D and G bands was calculated to be ( $I_D/I_G = 1.1844$ ). The morphological analysis carried out by transmission electron microscopy (TEM). Fig. 2 TEM images of *f*-MWCNTs with different magnifications, such as a=0.5  $\mu\text{m}$ , b=100, nm c=20 nm and d=10 nm. Herein, Figure. 2a shows that the bundles of nanotubes combined with each other with the scale of 0.5  $\mu\text{m}$ . Fig. 2b shows that the *f*-MWCNTs obtained length or long nanowires. (Figure. 2b, inset) shows that HRTEM image of *f*-MWCNTs, it clearly reveals amorphous nature. Figure. 2c and 2d shows that the different magnifications of *f*-MWCNT.

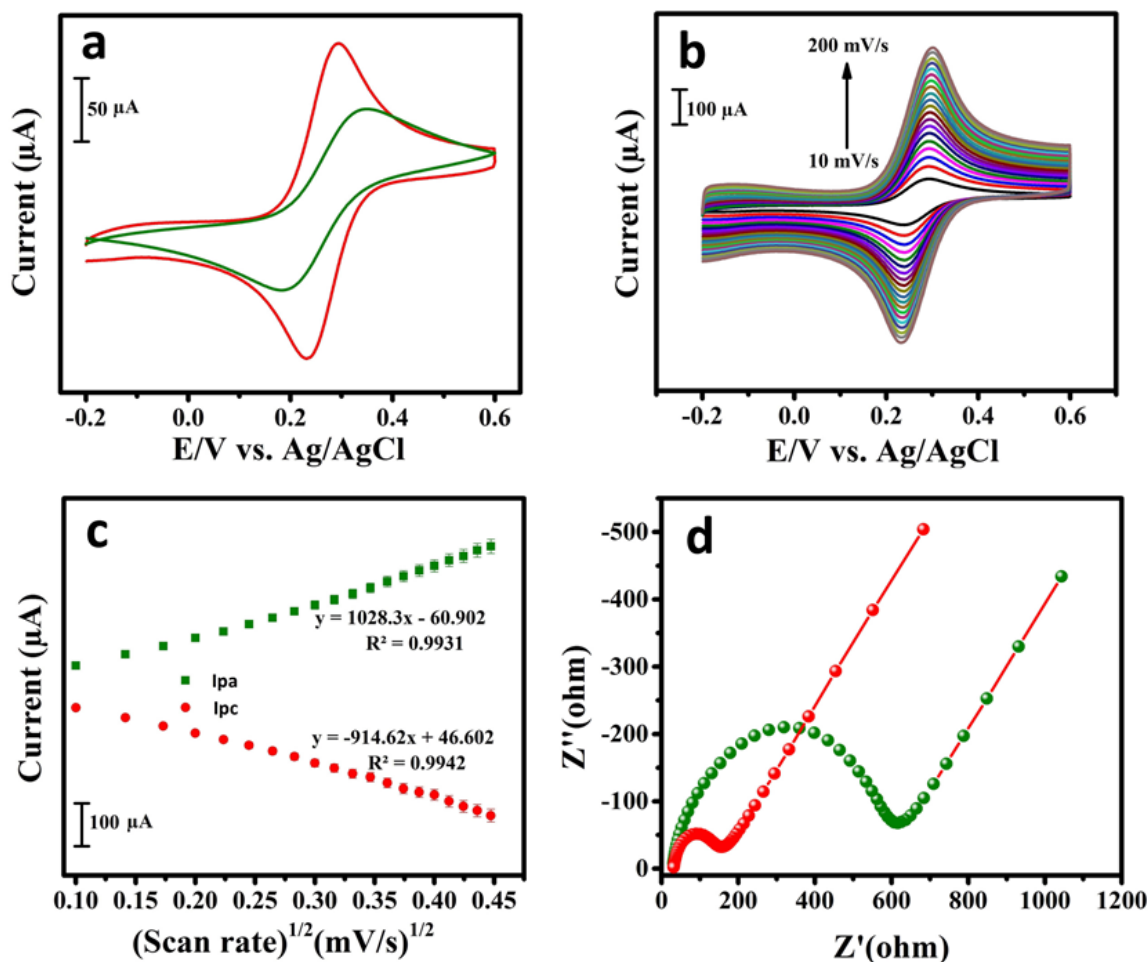


**Figure 3.** CV responses of bare GCE, GCE/*f*-MWCNTs and GCE/*f*-MWCNTs in 0.1 M KCl containing 5 mM  $[\text{Fe}(\text{CN})_6]^{3-/4-}$  (a) and the different scan rate from 10–200 mV/s (b), the corresponding plot of square root of scan rate vs. peak current (c) and EIS spectrum of the bare GCE, and GCE/*f*-MWCNTs recorded in 0.5 M KCl containing 0.005 M  $[\text{Fe}(\text{CN})_6]^{3-/4-}$  redox probe (d).

The electrochemical behavior of two different electrodes bare GCE and GCE/*f*-MWCNTs were studied in 0.5 M KCl bearing 0.005M of  $[\text{Fe}(\text{CN})_6]^{3-/4-}$  redox probe. Figure. 3a shows that the CV responses of bare GCE, and GCE/*f*-MWCNTs in  $[\text{Fe}(\text{CN})_6]^{3-/4-}$ , which exhibited that the pair of well-

defined redox peaks for the redox reaction of  $[\text{Fe}(\text{CN})_6]^{3-/4-}$ . However, the GCE/*f*-MWCNTs revealed a higher redox peak current and smaller peak-to-peak potential separation compared to the bare GCE. The peak-to-peak separations ( $\Delta E_p$ ) of different electrodes, bare GCE and GCE/*f*-MWCNTs are showed as 165.6 and 58.7 mV respectively.

The effective electrochemical active surface area of GCE/*f*-MWCNTs, the redox properties of GCE/*f*-MWCNTs was studied in  $[\text{Fe}(\text{CN})_6]^{3-/4-}$  at different scan rates ranging from 10 to 200 mV/s (Figure. 3b).

The electroactive surface area (EASA) of the modified electrode was calculated by the Randles–Sevcik equation. [29]

$$i_p = 2.69 * 10^5 n^{3/2} A D^{1/2} C \nu^{1/2}$$

Herein,  $i_p$ -peak current,  $n$ -number of electron transfer,  $A$ -electrochemical active area ( $\text{cm}^2$ ),  $D$  - diffusion coefficient ( $\text{cm}^2 \text{ s}^{-1}$ ),  $C$ -concentration of the  $[\text{Fe}(\text{CN})_6]^{3-/4-}$  molecules ( $\text{molL}^{-1}$ ), and  $\nu^{1/2}$  - scan rate ( $\text{V s}^{-1}$ ). From the slopes of the  $I_{pa}$  versus.  $\nu^{1/2}$ . (Figure. 3c) the EASA was calculated to be  $0.2756 \text{ cm}^2$  for GCE/*f*-MWCNTs. These results indicated that the GCE/*f*-MWCNTs have a high EASA. The electrochemical impedance spectroscopy (EIS) is an efficient technique to intrigue the electron transfer properties of surface modified GCEs. Figure. 3d. shows the EIS spectrum of the bare GCE, and GCE/*f*-MWCNTs recorded in 0.5 M KCl containing 0.005 M  $[\text{Fe}(\text{CN})_6]^{3-/4-}$  redox probe. The typical Nyquist plot of the GCE/*f*-MWCNTs exhibited the semicircle with a charge transfer resistance ( $R_{ct}$ ) of 0.1332  $\text{k}\Omega$ , this is quite smaller when compared with bare GCE (0.5806  $\text{k}\Omega$ ). However, the bare GCE revealed higher  $R_{ct}$  value of 0.5806  $\text{k}\Omega$  which implies that the bare GCE has high resistance. It can be noted that bare GCE created more resistance at electrode and electrolyte interface. These results are indicated that the GCE/*f*-MWCNTs have the excellent electrochemical properties than that of bare GCE.

**Table 1** Electrochemical active surface area ( $\text{cm}^2$ ) at different modified electrodes.

Electrode	Electrochemical active Surface area ( $\text{cm}^2$ )	Ref.
GCE <sup>a</sup> /GO <sup>b</sup>	0.003	30
GCE/NDC <sup>c</sup>	0.045	30
GCE/ <i>f</i> -MWCNTs <sup>d</sup>	0.2756	This work

<sup>a</sup>GCE- glassy carbon electrode, <sup>b</sup>GO- Graphene oxide, <sup>c</sup>NDC-Nitrogen doped carbon, <sup>d</sup>*f*-MWCNT

### 3.1 Electrochemical behavior of 4-NP

The electrocatalytic reduction of 4-NP on bare GCE and GCE/*f*-MWCNTs was predominantly evaluated by cyclic voltammetry. Figure. 4a a well-defined reduction peak appeared for the modified electrode (GCE/*f*-MWCNTs) and bare GCE at various peak potential ( $E_{pc2}$ ) -0.65,-0.82 for the

addition of 200  $\mu\text{M}$  4-NP, respectively. The appearance of a redox couple ( $E_{pa1} = 0.13\text{ V}$  and  $E_{pc1} = 0.08\text{ V}$ ) suggests that the reduction of 4-NP involves the transfer of  $4e^-$ , it leads to the constitution of 4-hydroxy aminophenol and the redox couple can be assigned to 4-hydroxyaminophenol/4-nitrosophenol. After concerns about different films, the modified electrodes more reactive compared to bare GCE.

Furthermore, the pH of the electrolytes (pH-3 to 11) significantly influenced the electrochemical behavior of 4-NP (200  $\mu\text{M}$ ), It can be seen that the peak potentials of the 4-NP reduction curves were shifted to the more negative potential when increasing the pH shown in Figure. 4b. The cathodic peak potentials ( $E_{pc}$ ) did not follow the linear relationship against the pH, which means the electrolytes influencing the electrocatalytic behavior of 4-NP and (Figure. 4b, inset) shows that the plot against different pH vs. peak current response.

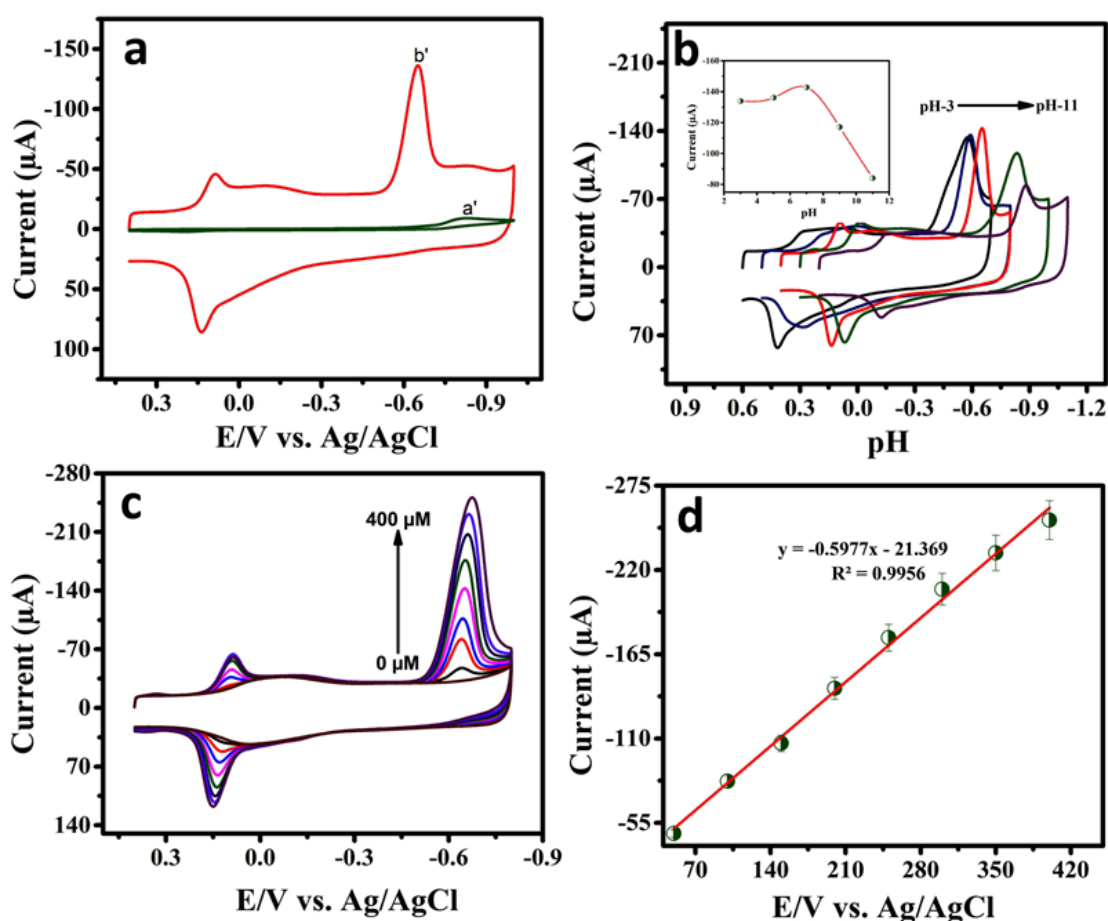


**Figure 4.** (a) The CVs of (a')bare GCE and (b') GCE/f-MWCNTs in 0.05 M PB solution, in the presence of 200  $\mu\text{M}$  4-NP. (b) The CV responses of 4-NP at GCE/f-MWCNTs in various pHs ranging from 3 to 11. The (inset 4b) shows that the plot against different pH vs. peak current response. (c) The CV curves of GCE/f-MWCNTs in various concentrations of 4-NP ranging from 0 to 400  $\mu\text{M}$  and (d) the corresponding plot of peak current vs. concentration of 4-NP.

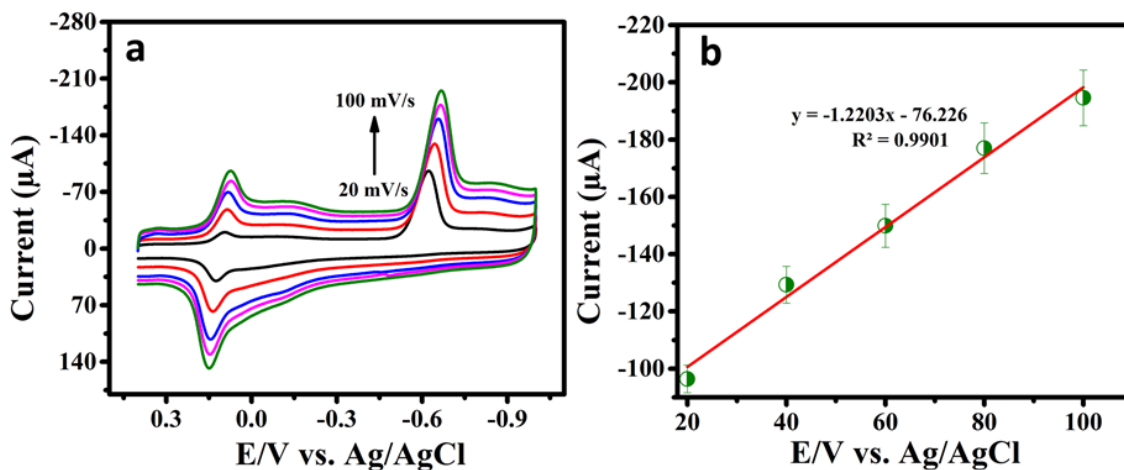


**Figure 5.** (a) The CV curves of GCE/f-MWCNTs in 0.05 M PB solution containing 200  $\mu\text{M}$  4-NP for the different scan rates ranging from 10 to 100 mV/s and (b) the corresponding plot of peak current vs. scan rate.

3.2 Effect of concentration and scan rate

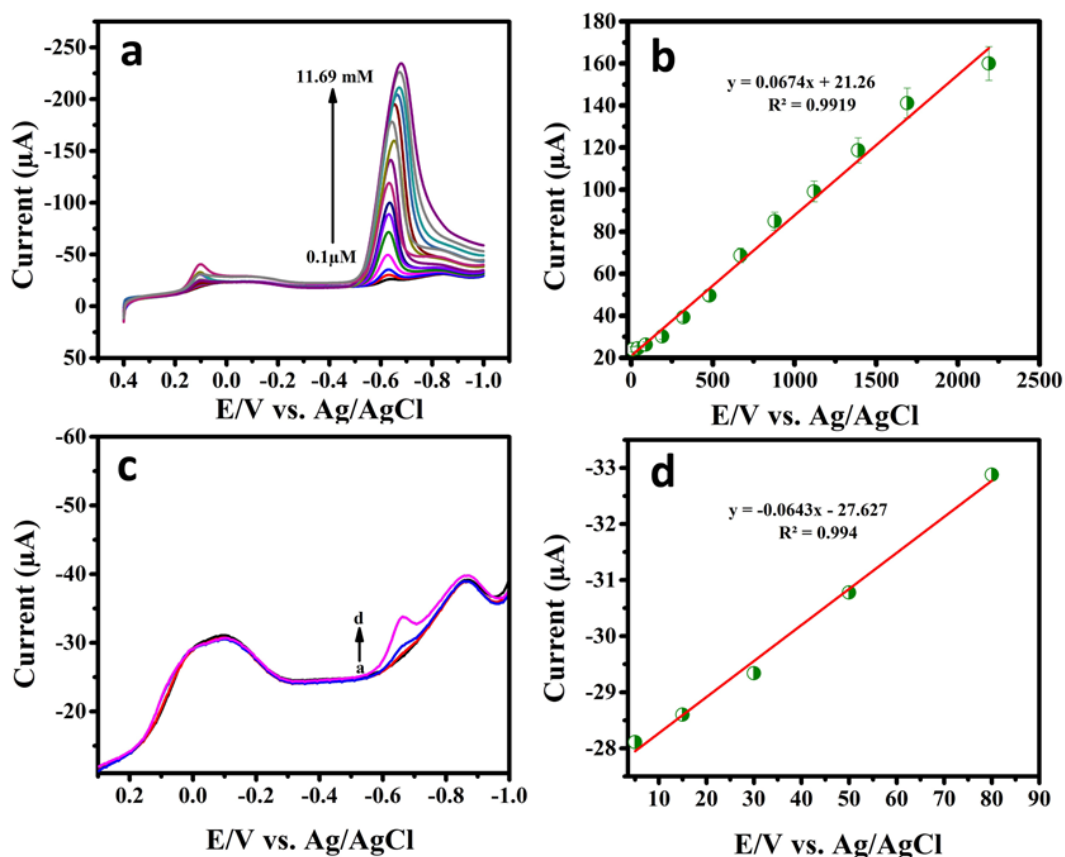


**Figure 6.** (a) The LSV responses of GCE/f-MWCNTs in various concentrations of 4-NP ranging from 0.1 to 2190  $\mu\text{M}$  in 0.05 M PB solution and (b) the corresponding calibration plot peak current vs. concentration of 4-NP. (c) Shows that the real sample analysis of 4-NP from laboratory tap water (LTW) and (d) the corresponding calibration plot peak current vs. concentration.

Figure. 4c shows the CV responses of the different addition of 4-NP (0-400  $\mu\text{M}$ ), which are recorded in 0.05 M phosphate buffer (PB) solution at a scan rate of 50 mV/s. Figure. 4d the corresponding plot of peak current vs. concentration of 4-NP. These results confirm that the 4-NP occur good linearity over the concentration of 0 to 400  $\mu\text{M}$ .

$$I_{pc}(\mu\text{A}) = -5.977 * 10^{-5} \left( \frac{\text{A}}{\text{Vs}^{-1}} \right) - 21.369 \quad (R^2 = 0.9956)$$

Moreover, the electrocatalytic behavior of 4-NP was studied by using cyclic voltammetry (CV). Figure 5a shows that the different scan (50 mV/s) rates in the presence of 4-NP. Figure. 5b shows that the different scan rates of 4-NP plotted against peak current vs. scan rate, respectively. Herein, 4-NP ensue good linearity at different scan rate (20 to 100 mV/s).

$$I_{pc}(\mu\text{A}) = -1.22 * 10^{-6} \left( \frac{\text{A}}{\text{Vs}^{-1}} \right) - 76.226 \quad (R^2 = 0.9901)$$

### 3.3 Determination of 4-NP on the modified electrode (GCE/f-MWCNT)

Linear sweep voltammetry is a sensitive tool to calculate the concentrations of 4-NP, herein, the LSV was used to determine the 4-NP. Figure. 6a shows the LSV responses of 4-NP reduction in the presence of 0.05 M PB (pH = 7) solution containing various concentrations of 4-NP from 0.1 to 2190  $\mu\text{M}$ . A sharp reduction peak has appeared for the addition of 0.1  $\mu\text{M}$  of 4-NP. The reduction peak currents were consecutively increased with increasing the concentrations of 4-NP. The observed reduction peak current was increased with increasing the concentrations of 4-NP ranging from 0.1 to 2190  $\mu\text{M}$  with  $R^2=0.9919$  shown in Figure. 6b. The detection limit was calculated to be 0.32  $\mu\text{M}$  with reliable sensitivity for the detection of 4-NP.[31-34] The comparison study of 4-NP sensors was described in the previous literature are given in Table 2.

**Table 2** The comparison for the electrocatalytic activity towards different modified electrodes for the detection of 4-NP.

Electrode materials	Detection limit ( $\mu\text{M}$ )	Linear range ( $\mu\text{M}$ )	Recovery (%)	References
GCE <sup>a</sup> /HN <sup>b</sup>	0.6	1.0–300	96–104	31
GCE/Silver particles	0.5	1.5–140	-	32
GCE/MWNTs <sup>c</sup>	0.4	2–4000	96–102	33
GCE/Ni–Co <sub>OX</sub> NPs <sup>d</sup>	4.8	7–682	101	34
GCE/f-MWNTs <sup>e</sup>	0.32	0.1-2190	97	(This work)

<sup>a</sup>GCE- glassy carbon electrode, <sup>b</sup>HN-hydroxyapatite Nano powder, <sup>c</sup>MWNT-Multi-wall Carbon Nanotubes, <sup>d</sup>f-MWNT- functionalized Multi Wall Carbon Nanotubes, <sup>e</sup>Ni–Co<sub>OX</sub> NPs- Nickel–Cobalt oxide nanoparticle.

### 3.4 Real sample analysis of 4-NP

The developed 4-NP sensor was evaluated laboratory tap water (LTW) towards the determination of 4-NP. Here, the experiment was performed by directly adding the LTW in 0.05 M PB solution and determined the concentrations of 4-NP. Figure. 6c shows the LSV responses of 4-NP determination in 0.05 M PB solution by adding the various amounts of LTW. Figure. 6d shows that the linear response of 4-NP detection on real sample analysis. It implies that the concentration of 4-NP gradually increasing with increasing the concentration of LTW which shows that the results were given in Table 3.

**Table 3** The real sample analysis of 4-NP from laboratory tap water (LTW) using LSV.

Sample	Added( $\mu\text{M}$ )	Found( $\mu\text{M}$ )	Recovery (%)
laboratory tap water(LTW)	5	4.87	97.4
	15	19.51	97.55
	30	48.74	97.48
	80	124.36	95.7

## 4. CONCLUSION

In summary, we have developing carbon materials for the sensors, batteries and supercapacitors applications. However, it has high conductivity and more surface area. The proposed GCE/*f*-MWCNTs modified electrode offers good EASA ( $0.2756 \text{ cm}^2$ ). In addition, we developed the modified (GCE/*f*-MWCNTs) electrode to detect the 4-NP from the water sample. The developed modified electrode gives good electrocatalytic activity towards the detection of 4-NP. The detection limit was calculated to be  $0.32 \mu\text{M}$  with reliable sensitivity. The developed sensor was analyzed by using laboratory tap water (LTW) for the detection of 4-NP, it gives acceptable recovery (97%), respectively.

## ACKNOWLEDGEMENTS

The project was supported by the Ministry of Science and Technology (MOST), Taiwan. This work also jointly supported by the projects from NTUT-NUST-107-1 and NSFC51572126, National Taipei University of Technology and Nanjing University of Science and Technology. This work was also supported by the National Natural Science Foundation of China (grant nos. 51572126)

## References

1. D.P. Zhang, W.L. Wu, H.Y. Long, Y.C. Liu and Z.S. Yang, *Int. J. Mol. Sci.*, 9 (2008) 316-326.
2. H. Yin, Y. Zhou, S. Ai, X. Liu, L. Zhu and L. Lu, *Microchim. Acta*, 169 (2010) 87-92.
3. Y. Sun, J. Zhou, W. Cai, R. Zhao and J. Yuan, *Appl. Surf. Sci.*, 349 (2015) 897-903.
4. Y.X. Yao, H.B. Li, J.Y. Liu, X.L. Tan, J.G. Yu and Z.G. Peng, *J. Nanomater.*, 2014 (2014) 84.

5. S. Hamidouche, O. Bouras, F. Zermane, B. Cheknane, M. Houari, J. Debord, M. Harel, J.-C. Bollinger and M. Baudu, *Chemical Engineering Journal*, 279 (2015) 964-972.
6. G. Bharath, V. Veeramani, S.M. Chen, R. Madhu, M.M. Raja, A. Balamurugan, D. Mangalaraj, C. Viswanathan and N. Ponpandian, *RSC Adv.*, 5 (2015) 13392-13401.
7. F. Karasek, S. Kim and H. Hill, *Anal. Chem.*, 48 (1976) 1133-1137.
8. F. Elbarbry, K. Wilby and J. Alcorn, *J. Chromatogr. B*, 834 (2006) 199-203.
9. M. Villar-Navarro, M. Ramos-Payán, J.L. Pérez-Bernal, R. Fernández-Torres, M. Callejón-Mochón and M.Á. Bello-López, *Talanta*, 99 (2012) 55-61.
10. A. Niazi and A. Yazdanipour, *J. Hazard. Mater.*, 146 (2007) 421-427.
11. L. Tarpani, E. Mencarelli, M. Nocchetti, L. Fano, L. Taglieri and L. Latterini, *Catal. Commun.*, 74 (2016) 28-32.
12. L. Guo, Z. Li, H. Chen, Y. Wu, L. Chen, Z. Song and T. Lin, *Anal. Chim. Acta*, 967 (2017) 59-63.
13. Y. Zhou, Z.b. Qu, Y. Zeng, T. Zhou and G. Shi, *Biosens. Bioelectron.*, 52 (2014) 317-323.
14. M.M. F. Chang, I. R. Ginjom and S. M. Ng, *Sens. Actuators, B*, 242 (2017) 1050-1056.
15. M.Miró, A. Cladera, J.M. Estela and V. c. Cerdà, *Anal. Chim. Acta*, 438 (2001) 103-116.
16. D. De Souza, L.H. Mascaro and O. Fatibello-Filho, *International journal of analytical chemistry*, 2011.
17. L. Chu, L. Han and X. Zhang, *J. Appl. Electrochem.*, 41 (2011) 687-694.
18. P. Deng, Z. Xu and J. Li, *Microchim. Acta*, 181 (2014) 1077-1084.
19. V.A. Pedrosa, L. Codognoto, S.A. Machado and L.A. Avaca, *J. Electroanal. Chem.*, 573 (2004) 11-18.
20. B. Yosypchuk and L. Novotný, *Crit. Rev. Anal. Chem.*, 32 (2002) 141-151.
21. Ø. Mikkelsen and K. H. Schrøder, *Electroanalysis*, 15 (2003) 679-687.
22. L. Hernández, P. Hernández and J. Vicente, *Fresenius J. Anal. Chem.*, 345 (1993) 712-715.
23. K. Krishnamoorthy, K. Jeyasubramanian, M. Premanathan, G. Subbiah, H. S. Shin and S. J. Kim, *Carbon*, 72 (2014) 328-337.
24. S. Radhakrishnan, K. Krishnamoorthy, C. Sekar, J. Wilson and S. J. Kim, *Appl. Catal., B*, 148 (2014) 22-28.
25. P. Xiao, F. Zhao and B. Zeng, *Microchem. J.*, 85 (2007) 244-249.
26. H. Luo, Z. Shi, N. Li, Z. Gu and Q. Zhuang, *Anal. Chem.*, 73 (2001) 915-920.
27. G. Rosace, V. Trovato, C. Colleoni, M. Caldara, V. Re, M. Bruciale, E. Piperopoulos, E. Mastronardo, C. Milone and G. De Luca, *Sens. Actuators, B*, 252 (2017) 428-439.
28. P. Han, Y. Yue, L. Zhang, H. Xu, Z. Liu, K. Zhang, C. Zhang, S. Dong, W. Ma and G. Cui, *Carbon*, 50 (2012) 1355-1362.
29. X. Chen, J. Zhu, Q. Xi and W. Yang, *Sens. Actuators, B*, 161 (2012) 648-654.
30. N. Karikalan, R. Karthik, S.M. Chen and H.A. Chen, *Sci. Rep.*, 7 (2017) 45924.
31. H. Yin, Y. Zhou, S. Ai, X. Liu, L. Zhu and L. Lu, *Microchim. Acta*, 169 (2010) 87-92.
32. I. G. Casella and M. Contursi, *J. Electrochem. Soc.*, 154 (2007) 697-702.
33. L.q. Luo, X.l. Zou, Y.p. Ding and Q.s. Wu, *Sens. Actuators, B*, 135 (2008) 61-65.
34. K. Asadpour-Zeynali and E. Delnavaz, *J. Iran. Chem. Soc.*, 14 (2017) 2229-2238.